IOP PUBLISHING JOURNAL OF PHYSICS D: APPLIED PHYSICS

J. Phys. D: Appl. Phys. **46** (2013) 065310 (9pp) doi:10.1088/0022-3727/46/6/065310

High- and low-energy x-ray photoelectron techniques for compositional depth profiles: destructive versus non-destructive methods

Noelia Benito[1], Ramón Escobar Galindo[2], Juan Rubio-Zuazo[2,3], Germán R Castro[2,3] and Carlos Palacio[1]

[1] Departamento de Física Aplicada, Facultad de Ciencias, Módulo 12. Universidad Autónoma de Madrid, Cantoblanco, 28049-Madrid, Spain
[2] Instituto de Ciencia de Materiales de Madrid, Consejo Superior de Investigaciones Científicas, Cantoblanco, 28049-Madrid, Spain
[3] SpLine Spanish CRG Beamline at The ESRF, BP 220, 38043 Grenoble cedex, France

E-mail: carlos.palacio@uam.es (C Palacio)

Received 15 October 2012, in final form 12 December 2012
Published 17 January 2013
Online at stacks.iop.org/JPhysD/46/065310

Abstract
Hard x-ray photoelectron spectroscopy (HAXPES), angle-resolved x-ray photoelectron spectroscopy (ARXPS) and x-ray photoelectron spectroscopy (XPS) with simultaneous Ar^+ bombardment are used to obtain chemical information and concentration depth profiles of thin film oxides on Cr, Al, Si substrata and to explore the capabilities of analyzing buried interfaces at depths above 10 nm in Cr–O–Al thin films mixed oxides deposited on Si substrata. ARXPS and HAXPES are non-destructive techniques and within the photon energy range (7.5–15 keV) and the emission angle range (0°–70°) used, both techniques provide equivalent information, ARXPS being more sensitive to the surface morphology. XPS and simultaneous sputtering with Ar^+ is a destructive technique and effects such as atomic mixing are unavoidable; however, the comparative study with HAXPES allowed the measurement of key parameters for the understanding of the ion–matter interaction such as the mixing extent and the interface broadening.

(Some figures may appear in colour only in the online journal)

1. Introduction

The chemical and compositional analysis of the near-surface region of solids and of very thin films can be carried out using either non-destructive or destructive methods depending on the thicknesses to be analysed. Actually, for thin films above 10 nm the method most frequently applied to obtain the concentration depth profiles (CDPs), that is, the thin film composition with depth is ion sputtering in combination with any of the surface analysis techniques [1, 2]. Among them AES, x-ray photoelectron spectroscopy (XPS) and SIMS are becoming the most popular. The choice of a specific technique depends on the concrete analytical problem to be solved although the general trend is the simultaneous use of several techniques due to the complementary information provided [1]. The main drawback of this approach is related to the surface modifications produced during ion bombardment since the sputtering process itself can alter the surface composition, the surface chemistry and morphology because of the different physical processes taking place during ion bombardment as preferential sputtering, enhanced induced diffusion processes, atomic mixing [1], etc. However, it has recently been shown that cluster ion beams minimize the accumulation of beam induced damage in a wide variety of organic materials [3].

Rutherford backscattering spectrometry (RBS) has also been used as a non-destructive method to obtain CDP. However, RBS does not provide chemical information and the depth resolution obtained is rather poor.

Other alternative non-destructive methods to obtain CDP are based on the use of XPS in conjunction with the control of the information depth. The information depth depends on the kinetic energy of the emitted photoelectrons and on its take off angle [4, 5]. Conventional XPS laboratory equipment ordinarily uses Mg or Al Kα (1253.6 or 1486.6 eV, respectively for the photon energy) and experimental setup allowing take off angle modifications from 0° to 70°. As an example, for Si 2p photoelectrons, assuming that the information depth is three times the attenuation length of the emitted photoelectrons, an information depth up to 8.2 nm can be obtained when Mg Kα is used as radiation. The variation of take off angle is named angle-resolved x-ray photoelectron spectroscopy (ARXPS) and therefore is useful for analysing in a non-destructive sense the very near surface of solids and very thin films [5]. The integral equation relating measured intensities as a function of the take off angle and the CDPs is a prototype of ill-posed problems and different approaches have been proposed to obtain the CDP from experimental measurements [5–7].

The kinetic energy of emitted photoelectrons and, as a consequence, the information depth can be increased using high brilliance synchrotron radiation sources. Recently, it has been shown in an experiment carried out at the Spanish CRG Spline beam line at the ESRF, Grenoble, France, that an information depth of 50 nm can be achieved detecting photoelectrons with 15 keV kinetic energy [8]. The technique is named hard x-ray photoelectron spectroscopy (HAXPES), it is also a non-destructive one and its capabilities are restricted by the limits imposed by the high electron energy analysers in such a way that only few synchrotron radiation facilities in the world allow experiments using that approach [8–11]. Further details on experimental and theoretical aspects of the technique can be obtained in [8–13].

Also, in-depth profile information on the near surface of the material can be obtained from the inelastic background that appears at the high binding energy side of the photoelectron peaks. Tougaard [14] has used this analysis to develop models that correlate the shape (inelastic background and elastic contributions) of photoelectron peaks with the in-depth profile that generates them.

The purpose of this work is to explore the capabilities of HAXPES to obtain the CDP either of buried interfaces or of thin films to characterize Cr, Al, Si thin film oxides as well as Cr–O–Al thin films mixed oxides through a comparative study using ARXPS, XPS and simultaneous sputtering, and HAXPES. As we have shown in previous works, Cr–O–Al and Cr–O–Si thin film mixed oxides are materials of technological interest since the refractive index of the film can be controlled through the composition control [15, 16].

2. Experimental

Two types of samples were analysed: (1) Cr, Al and Si native oxide films grown on bulk substrata and (2) mixed Cr–O–Al oxide thin films deposited on Si (1 0 0) substrates by dc magnetron sputtering using chromium/aluminium compound targets with relative percentage atomic ratios of Cr/Al = 10/90 in a high-purity (99.999%) argon and oxygen atmosphere. The sputtering chamber was pumped down to a base pressure below 8.6×10^{-4} Pa before letting in the gas mixture. The sputtering time was always kept fixed at 30 min and the oxygen flux was 5 sccm leading to a film thickness of 15 ± 3 nm as was determined with a Veeco Dektak 150 stylus surface profiler by measuring the height of a step left by a mechanical mask. Further experimental details on the mixed oxide deposition are given elsewhere [16].

For ARXPS measurements, the sample was placed in a sample stage with four degrees of freedom in such a way that the emission angle can be varied between 0° and 70° and XPS spectra were measured in an ultrahigh vacuum system at a base pressure below 8×10^{-8} Pa using a hemispherical analyser (SPECS Phoibos 100 MCD-5). The pass energy was 9 eV giving a constant resolution of 0.9 eV. The Au $4f_{7/2}$, Ag $3d_{5/2}$ and Cu $2p_{3/2}$ lines of reference samples at 84.0 eV, 368.3 eV and 932.7 eV, respectively, were used to calibrate binding energies. A twin anode (Mg and Al) x-ray source was operated at a constant power of 300 W using Mg Kα radiation. For depth profiling, ion bombardment was carried out using a penning ion source (SPECS IQP 10/63) with an angle of 45° between the normal to the surface and the ion gun axis, and an ion beam energy of 3 keV, increasing the pressure to 4×10^{-2} Pa of Ar^+. The ion beam current density, measured with a collector that can be placed in the same position as the sample holder, was $4.6\,\mu A\,cm^{-2}$. Those experimental conditions led to an ion beam with a flat profile greater than $\sim 10 \times 10\,mm^2$.

HAXPES analyses of these samples were performed at the Spanish CRG SpLine beamline (BM25) of the ESRF, Grenoble, France [9], using a sector of a cylindrical mirror analyser (HV-CSA300) [12, 17] enabling working in a very broad kinetic energy range (from few eV up to 15 KeV). A two-dimensional event counting detector was used in combination with the CSA analyser to reduce the counting rate. The analyser was used with a constant energy resolution of 1 eV in order to enhance the analyser transmission and to measure the photoemission spectra in few minutes. It should be indicated that high energy resolution is essential for an electronic depth profile but not for a compositional depth profile. The overall instrumental energy resolution results from the convolution of the analyser resolution with the x-ray bandwidth. For the present experiment a double crystal monochromator equipped with Si (1 1 1) crystals was used providing an energy resolution of $\Delta E/E = 1.5 \times 10^{-4}$. Photon energies from 7.5 to 16.4 keV were used to excite Cr 1s, Al 1s and Si 1s signals of the samples (from the oxide films and the substrata). The HAXPES measurements were performed in a geometry in which the direction of the x-rays, the photoelectron direction towards the analyser and the surface normal are in the x-ray polarization plane (azimuthal angle set to 0°). The photon incident angle was set to 5° with respect to the sample surface. The electron emission angle was fixed to 15°, on the forward direction, from the normal to the sample surface. Hence the angle formed between the x-rays direction and the analyser was 100°.

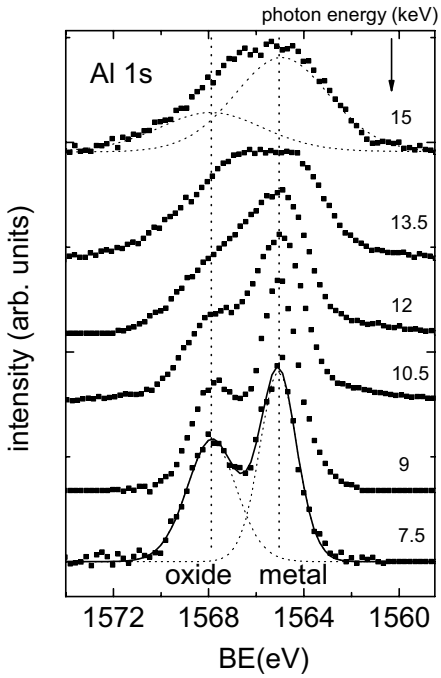

Figure 1. HAXPES Al 1s core level spectra as a function of the binding energy measured using different photon energies from 7.5 to 15 keV for the native Al oxide on an Al substrate.

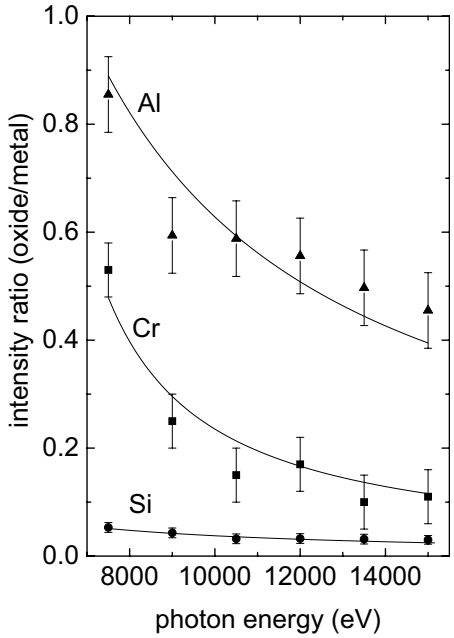

Figure 2. Intensity ratio $I_{\text{oxide}}/I_{\text{Metal}}$ derived from figure 1 for the native Al thin film oxide on Al (full triangles) as well as such ratios for the Cr (full squares) and Si (full circles) thin film oxides as a function of the photon energy. The oxide thicknesses obtained using equation (3) are $d_{\text{AlOxide}} = 7.83 \pm 0.5$ nm, $d_{\text{CrOxide}} = 1.71 \pm 0.09$ nm and $d_{\text{SiOxide}} = 0.93 \pm 0.13$ nm.

The AFM images were taken in air using a Nanotec microscope in tapping mode with SiN cantilevers provided by Olympus. Different size images were recorded, all of them with a resolution of 256 × 256 pixels.

3. Results and discussion

3.1. Thin oxide films

Figure 1 shows the Al 1s core level spectrum as a function of the binding energy measured using different photon energies from 7.5 to 15 keV for the native Al oxide on an Al substrate. The background was subtracted using a modified Shirley method [18, 19] and all the spectra were normalized to their areas. Similar results were obtained for the native Cr oxide and Si oxide on Cr and Si substrata. Results of figure 1 display two bands at 1565.0 and 1567.8 eV which are attributed to the metallic and oxidized species, respectively. As observed in figure 1 the full-width at half-maximum (FWHM) of both bands increases with increasing photon energy, as expected from a double crystal monochromator, in such a way that both features remain partially unresolved for photon energies above 12 keV.

Figure 2 shows the intensity ratio $I_{\text{oxide}}/I_{\text{Metal}}$ derived from figure 1 for the native Al thin film oxide on Al (full triangles) as well as such ratios for the Cr (full squares) and Si (full circles) thin film oxides as a function of the photon energy. As can be seen, a decrease in that ratio is observed with increasing photon energy, that is, with increasing the sampled depth. The depth profile of constituent elements of the substrate and overlayer film can be obtained from results of figure 2. To carry out this task a model has to be chosen for the overlayer oxide film, either islands or uniform film. For the island model the photoemission intensity for photoelectrons produced from a constituent element in the oxide layer is given by the parametric model described in [5] by equation (1)

$$I_{\text{oxide}} = I^{\infty}_{\text{oxide}}\theta\left[1 - \exp\left(\frac{-d}{\text{EAL}(E_{\text{kin}})\cos\varphi}\right)\right], \quad (1)$$

where $I^{\infty}_{\text{oxide}}$ is the intensity for the pure bulk oxide, θ is the island coverage, d is the island thickness, φ is the emission angle given by the experimental conditions and $\text{EAL}(E_{\text{kin}})$ is the effective attenuation length for the photoelectrons coming from the oxide islands. Similarly, the photoemission intensity for photoelectrons produced from a constituent element in the metallic substrate is given by

$$I_{\text{metal}} = (1-\theta)I^{\infty}_{\text{metal}} + \theta I^{\infty}_{\text{metal}}\exp\left(\frac{-d}{\text{EAL}(E_{\text{kin}})\cos\varphi}\right). \quad (2)$$

Since oxide and metallic photoelectrons have very similar kinetic energies and both are travelling through the oxide film, the same effective attenuation length values are used in both equations. The intensity ratio is then given by

$$\frac{I_{\text{oxide}}}{I_{\text{metal}}} = \frac{I^{\infty}_{\text{oxide}}}{I^{\infty}_{\text{metal}}}\,\frac{\left[1 - \exp\left(\frac{-d}{\text{EAL}(E_{\text{kin}})\cos\varphi}\right)\right]}{\left[\frac{1-\theta}{\theta} + \exp\left(\frac{-d}{\text{EAL}(E_{\text{kin}})\cos\varphi}\right)\right]} \quad (3)$$

in such a way that the limit case $\theta = 1$ provides the intensity ratio for the uniform film case.

The intensity ratio $I^{\infty}_{\text{oxide}}/I^{\infty}_{\text{metal}}$ can be calculated enough accurately using

$$\frac{I^{\infty}_{\text{oxide}}}{I^{\infty}_{\text{metal}}} = \frac{N_{\text{oxide}}\lambda_{\text{oxide}}}{N_{\text{metal}}\lambda_{\text{metal}}}, \quad (4)$$

Table 1. Summary of numerical values.

Material	SiO_2	Si	Cr_2O_3	Cr	Al_2O_3	Al
ρ (g cm^{-3})	2.65	2.33	5.21	7.19	3.86	2.70
N_{oxide} or N_{metal} (cm^{-3})	0.044	0.083	0.069	0.138	0.076	0.100
$\frac{\lambda_{oxide}}{\lambda_{metal}}$	1.22		1.13		1.06	
$\frac{I^{\infty}_{oxide}}{I^{\infty}_{metal}}$	0.65		0.57		0.81	

Table 2. Best fit parameters for the HAXPES and ARXPS results of figures 2 and 4.

	Al	Cr	Si
HAXPES			
Coverage (θ)	1	1	1
Film thickness (nm)	7.83 ± 0.50	1.71 ± 0.09	0.93 ± 0.13
ARXPS			
Coverage (θ)	0.94 ± 0.01	0.91 ± 0.01	1
Film thickness (nm)	7.29 ± 0.27	2.52 ± 0.06	1.64 ± 0.04

where N_{oxide} is the atomic density of metal in the oxide, N_{metal} for pure metal and the λ values are the inelastic mean free paths (IMFPs) for electrons from metal in oxide and from metal in metal, respectively. Values of N for metals are known accurately which is not completely true for oxides. The oxide bulk densities ρ used to calculate the N values for the oxides are taken from [20] and are given in table 1 along with the calculated atomic densities. The $\lambda_{oxide}/\lambda_{metal}$ ratio is calculated according to the approach TPP-2M of Tanuma *et al* [21] and the values are also given in table 1.

Experimental results of figure 2 are fitted to the model of equation (3) using the IMFPs also calculated from Tanuma *et al* [21] in the appropriate energy range for the emitted photoelectrons (photon energies are in the range 7.5–15 keV). We have used here the IMFPs instead of the EAL since at the high kinetic energies used, the values of the corresponding EALs and IMFPs do not deviate significantly due to the weak influence of elastic scattering. It should be pointed out that the best fit was always reached in the limit case of $\theta = 1$, that is, assuming a uniform oxide film on the substrate and therefore this parameter was fixed. The only fitting parameter was the thickness of the film d. The best fit parameters are given in table 2, and the results of the fitting are shown in figure 2 using continuous lines. As can be observed, the fitting is fairly good, indicating that HAXPES is a useful tool to obtain the CDP of thin oxide films on a substrate.

The second strategy to obtain the CDP of very thin oxide films is based on the use of conventional XPS (with Mg or Al kα radiation) in conjunction with the variation of the emission angle φ (ARXPS) to control of the information depth. As pointed out before, for such experimental setup, information depths of ~8.2 nm can be reached for Si and therefore, looking at results of table 2 for HAXPES, ARXPS should be also a useful tool for analysing native oxide films on Al, Cr and Si. The use of ARXPS should be also a valuable test for comparison purposes.

Figure 3 shows the Al 2p bands as a function of the binding energy for different emission angles from 0° to 70° measured on the same sample of figure 1. Again, the background was subtracted using a modified Shirley method [18, 19] and all the spectra were normalized to their areas. Similar results were obtained for the native Cr oxide and Si oxide on Cr and Si substrata. The Al 2p band was characterized by two peaks at 71.5 eV and 74.5 eV that are attributed to metallic and oxidized species, respectively [22]. As can be observed, the intensity associated with the metallic band clearly decreases with increasing the emission angle, whereas that associated with the oxide remains nearly constant.

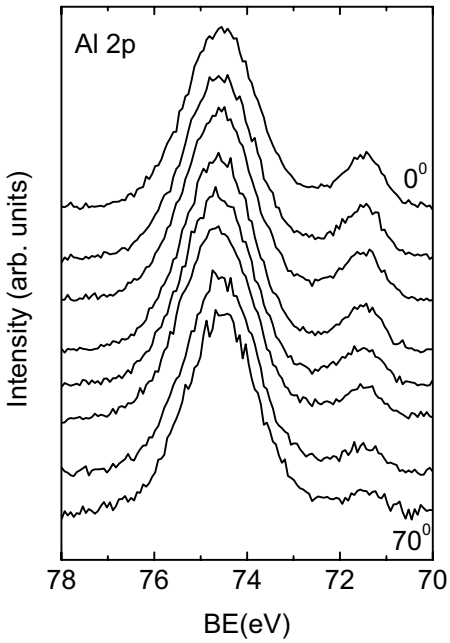

Figure 3. Al 2p spectra as a function of the binding energy for different emission angles from 0 to 70° measured on the same sample of figure 1. The background is subtracted using a modified Shirley method (see references in the text).

Figure 4 shows the intensity ratio I_{oxide}/I_{Metal} derived from figure 3 for the native Al thin film oxide on Al (full triangles) as well as such ratios for the Cr (full squares) and Si (full circles) thin film oxides as a function of the emission angle. It is worth noting that the intensity ratio strongly increases with increasing emission angle, that is, with decreasing the sampled depth, therefore indicating the high surface sensitivity of the technique. The depth profile of constituent elements of the substrate and overlayer film can be obtained from the results of figure 4 using equation (3) as for HAXPES. The fitting parameters are now the coverage, θ, and the thickness, d, and the accuracy of the calculated thickness depends on the accuracy of the EAL values used. In general, equation (3) can be used with EAL calculated from the IMFP reduced for elastic scattering and considering that for most practical measurement conditions the reduction factor is around 0.9 [23]. Therefore, experimental results of figure 4 were fitted to the model of equation (3) using the corrected IMFP calculated using TPP-2M [21]. The best fit parameters are also given in table 2 and the results of the model are represented in figure 4 by continuous lines. It should be indicated that for Si the best fitting led to coverage values around 1.3, therefore the constraint $\theta \leqslant 1$

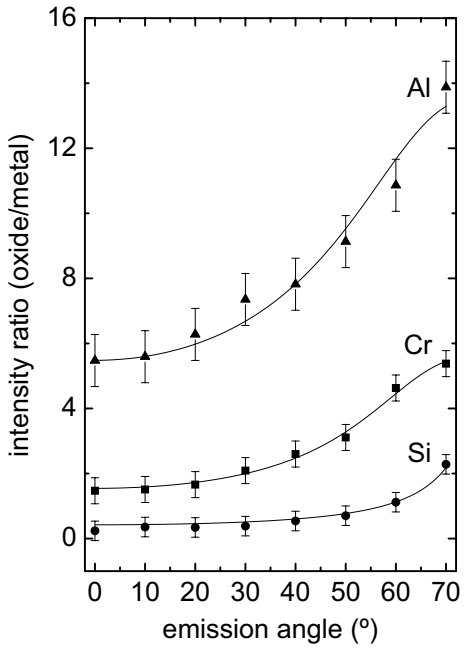

Figure 4. Intensity ratio $I_{\text{oxide}}/I_{\text{Metal}}$ derived from figure 3 for the native Al thin film oxide on Al (full triangles) as well as such ratios for the Cr (full squares) and Si (full circles) thin film oxides as a function of the emission angle. The calculated oxide thicknesses are $d_{\text{AlOxide}} = 7.29 \pm 0.27$ nm, $d_{\text{CrOxide}} = 2.52 \pm 0.06$ nm and $d_{\text{SiOxide}} = 1.64 \pm 0.04$ nm.

was imposed in order to have a meaningful physical results. As observed in table 2 the results obtained by HAXPES are somewhat different from those obtained by ARXPS. Merzlikin *et al* [24] pointed out that the roughness of the analysed surface plays an important role to explain such differences since the roughness of the surface smoothes out the angular dependence of intensities, which results in underestimation of the layer thickness. In our case, results of table 2 indicate that this is true for the Al oxide film but not for the Cr and Si oxides. In order to find a possible explanation, AFM measurements were carried out on the oxide film surfaces. Figure 5 shows the AFM images of the surface of the oxides films on Si, Cr and Al along with some line scans indicated on the images. For Si the surface level fluctuates between 2 and 10 nm displaying a background rather flat. The Cr surface displays grain boundaries and a non-flat background being the stronger oscillation between 45 and 85 nm. Finally, the line scan corresponding to the Al image displays strong oscillations up to 200 nm. Although for the moment the influence of the surface morphology on the measured thickness is not well understood, obviously such complicated and different surface morphologies should influence quantitative results and therefore additional works are necessary to clarify this point. Anyway, ARXPS measurements are more affected by surface morphology than HAXPES measurements where the geometry is not changed [24].

3.2. *Buried interfaces*

Finally, HAXPES was used to probe the interface Cr–O–Al mixed oxide/Si. We have shown recently [16] that Cr–O–Al thin film mixed oxides grown on Si (1 0 0) substrates by reactive magnetron sputtering are useful technological materials. From the chemical information obtained with XPS as well as the observed chemical shift of the Cr 2p, Al 2s and O 1s bands we concluded in that publication the formation of mixed substitutional Me_2O_3 oxides (Me= Al+Cr) instead of the formation of single oxide phases for a broad range of target compositions from 90% Cr (10% Al) to 10% Cr (90% Al) which was confirmed through the compositions and stoichiometries obtained from CDPs measured using simultaneously XPS and Ar^+ bombardment. Moreover, the optical properties of the films such as their refractive index are controlled through their chemical composition [16] and therefore, the correct characterization of the film and interfaces is an important matter.

Figure 6 shows the measured intensities-sputter time profile of a thin Cr–O–Al mixed oxide film (target composition Cr = 10%, Al = 90%) grown on Si measured using simultaneously XPS and Ar^+ bombardment at 3 keV. The buried Si oxide interface and the Si substrate are also shown. The mixed oxide film displays (not shown) uniform composition (O 62%, Al 36% and Cr 2%). For further information on the film composition and optical properties see [16]. As pointed out in the experimental part, a film thickness of 15 ± 3 nm was determined with a Veeco Dektak 150 stylus surface profiler by measuring the height of a step left by a mechanical mask. The raw data consist of the elemental signal intensities as a function of the sputtering time. For quantification, the elemental intensities can be converted to the elemental concentrations using the sensitivity factors provided by the manufacturer [1, 16, 25]. Assuming constant the primary-ion current density, the sputtering yield and the atomic density of the eroded film and considering that the interface is determined at 50% [2] of the Si intensity ($t_{1/2}$), a constant sputtering rate of 0.38 ± 0.08 nm min^{-1} is obtained.

Complementary information on the above interface is obtained using HAXPES. Figure 7 shows the intensity ratios $I_{\text{AlOxide}}/I_{(\text{Si+SiOxide})}$ (full squares) and $I_{\text{SiOxide}}/I_{\text{Si}}$ (full circles) measured using HAXPES as a function of the photon energy for the same sample of figure 6. Looking at depth profile results of figure 6 such ratios should be modelled by a single Al mixed oxide layer on the substrate (SiOxide + Si) and by a buried silicon oxide layer between the Al mixed oxide layer and the Si substrate, respectively. The inset of figure 6 shows a schematic diagram of the films indicating the different thicknesses involved. Therefore, the equations of the parametric model can be written as

$$\frac{I_{\text{SiOxide}}}{I_{\text{Si}}} = \frac{I^{\infty}_{\text{SiOxide}}}{I^{\infty}_{\text{Si}}}\left[\exp\left(\frac{d_{\text{SiOxide}}}{\text{EAL}^{\text{SiOxide}}_{\text{Si}}}\right) - 1\right], \tag{5}$$

$$\frac{I_{\text{AlOxide}}}{I_{\text{Si}}} = \frac{I^{\infty}_{\text{AlOxide}}}{I^{\infty}_{\text{Si}}}\left[1 - \exp\left(-\frac{d_{\text{AlOxide}}}{\text{EAL}^{\text{AlOxide}}_{\text{Al}}(E_{\text{kin}})\cos\varphi}\right)\right] \times \exp\left(\frac{d_{\text{AlOxide}}}{\text{EAL}^{\text{AlOxide}}_{\text{Si}}(E_{\text{kin}})\cos\varphi}\right) \times \exp\left(\frac{d_{\text{SiOxide}}}{\text{EAL}^{\text{SiOxide}}_{\text{Si}}(E_{\text{kin}})\cos\varphi}\right). \tag{6}$$

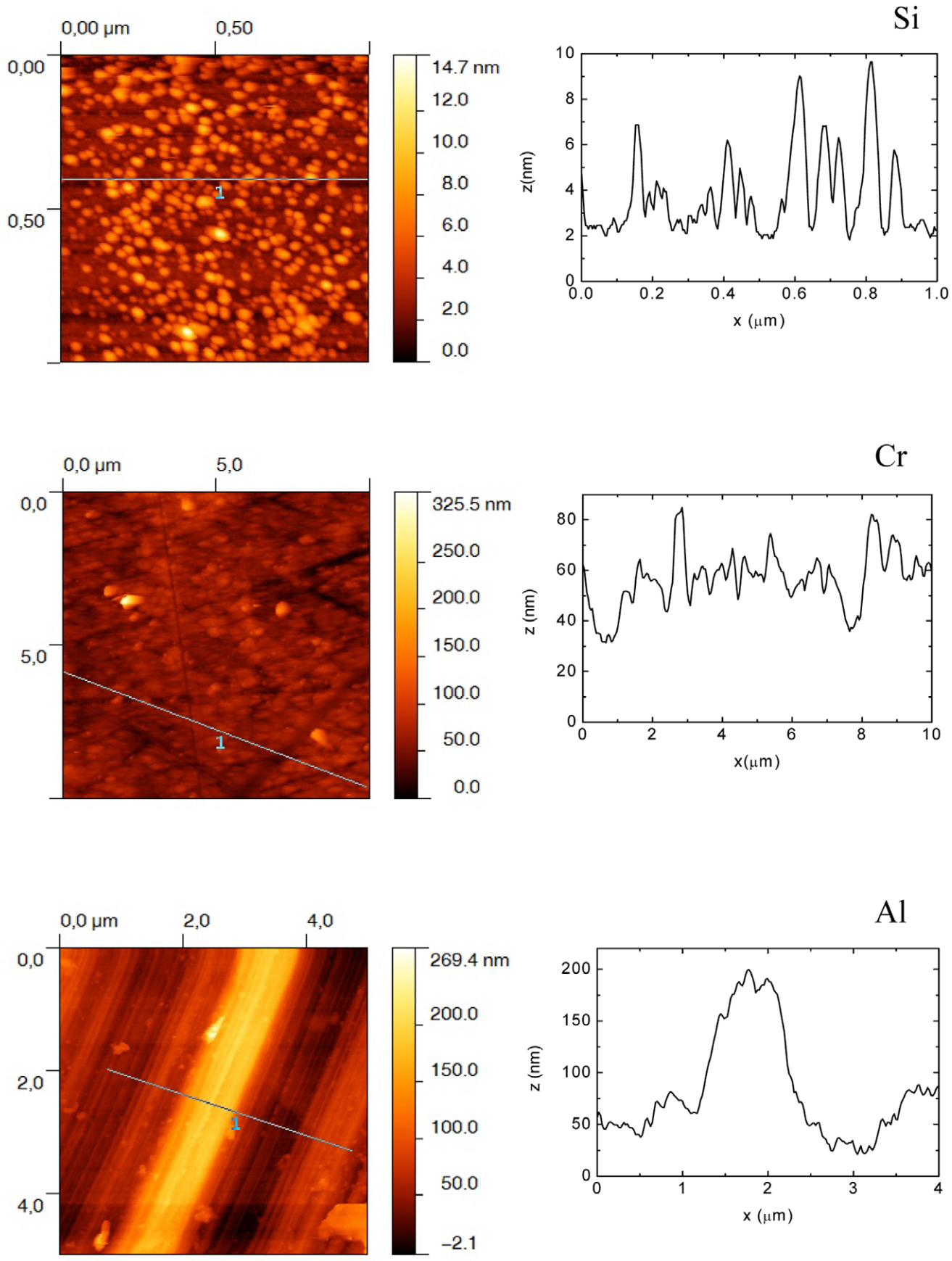

Figure 5. AFM images and line scans of (*a*) Si, (*b*) Cr and (*c*) Al surfaces.

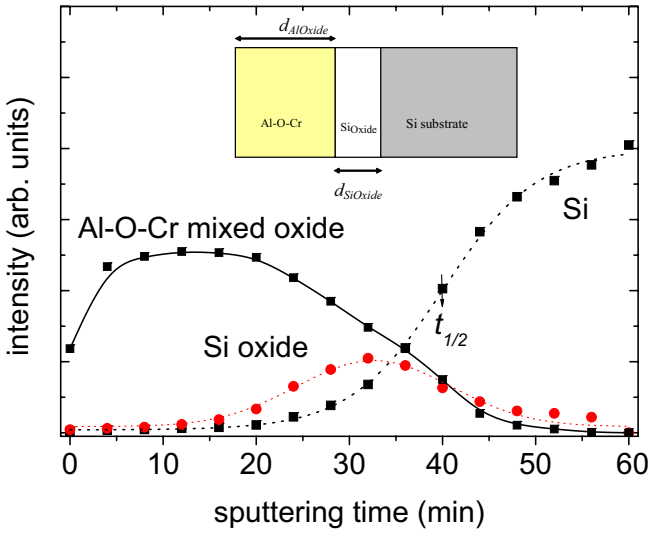

Figure 6. Depth profile for the Cr–O–Al mixed oxide film (target composition Cr = 10%, Al = 90%) grown on Si measured simultaneously using XPS and Ar^+ bombardment at 3 keV: Al species (full triangles), Si oxide species (open circles) and Si species (full circles). The position of the Si substrate interface which is determined at 50% of the Si intensity ($t_{1/2}$) was indicated by an arrow. The inset represents the schematic diagram of the film model.

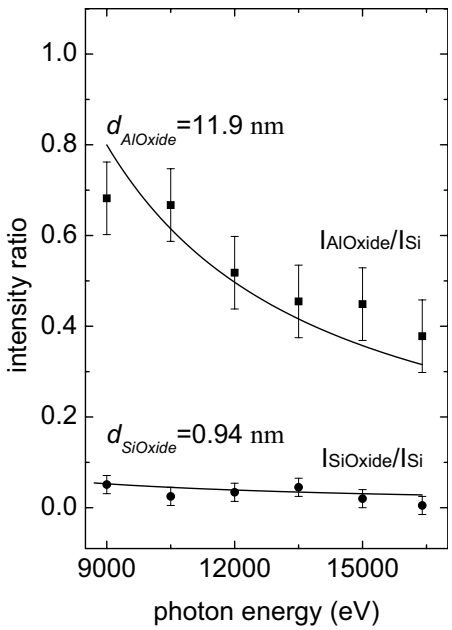

Figure 7. Intensity ratios $I_{AlOxide}/I_{(Si+SiOxide)}$ (full squares) and $I_{SiOxide}/I_{Si}$ (full circles) measured using HAXPES as a function of the photon energy for the same sample of figure 6.

Here EALs are the effective attenuation lengths, being the subscript indicative of the element producing the photoelectrons and the superscript of the material through which the photoelectrons are travelling. Experimental $I_{SiOxide}/I_{Si}$ intensity ratio is fitted to equation (5) using $d_{SiOxide}$ as fitting parameter. Again, we have used the IMFPs instead of the EAL since at the high kinetic energies used both values do not deviate significantly due to the weak influence of elastic scattering. The ratio $I^{\infty}_{SiOxide}/I^{\infty}_{Si}$ is calculated using equation (4) and the numerical values are given in table 1. The best fitting parameter is $d_{SiOxide} = 0.94 \pm 0.13$ nm. The result of the fitting is given in figure 7 by a continuous line. As can be observed, the agreement is very good.

Once $d_{SiOxide}$ is calculated, we have used equation (6) to calculate $d_{AlOxide}$. A difficulty in applying equation (6) is related to the uncertainties in the calculation of the $I^{\infty}_{AlOxide}/I^{\infty}_{Si}$ ratio. We have used equation (4) taking into account two considerations: the molecular densities of Al_2O_3 (0.038 mol cm^{-3}) and Cr_2O_3 (0.034 mol cm^{-3}) are very similar and the Al–O–Cr mixed oxide is a substitutional Me_2O_3 oxide (Me = Al + Cr) with only 1 Al atom per molecule [16]. Calculations within these conditions give

$$\frac{I^{\infty}_{AlOxide}}{I^{\infty}_{Si}} = 0.458\frac{\lambda^{oxide}_{Al}}{\lambda^{Si}_{Si}}. \qquad (7)$$

The best fitting between experimental data and equation [6] was obtained for $d_{Al} = 11.9 \pm 0.5$ nm and is represented by a continuous line in figure 7. It should be indicated that the thickness $d_{SiOxide}$ of the silicon oxide layer was fixed to the value 0.94 nm calculated previously. The very good agreement between theoretical and experimental results strongly supports the validity of the proposed film model and of the hypothesis used to calculate the $I^{\infty}_{AlOxide}/I^{\infty}_{Si}$ ratio.

At this point a comparison between the depth profile of figure 6, obtained by conventional XPS and simultaneous ion milling, and results of figure 7 is compulsory. Related to the measured thicknesses, 15 ± 3 nm as determined with stylus techniques and 11.9 ± 0.5 nm as determined from figure 7, the agreement is good enough within the accuracy provided by the stylus technique. It is worth noting that considering the estimated sputtering rate of 0.38 ± 0.08 nm min^{-1}, the thickness of the Si oxide layer in the interface between the Al–O–Cr oxide and the Si substrate, calculated from the FWHM of the Si oxide depth profile of figure 6, is 8.2 nm. This value is nearly an order of magnitude higher than that determined by HAXPES results of figure 7, that is, $d_{SiOxide} = 0.94$ nm. Moreover, the interface broadening which corresponds to the difference of the depth coordinate between 84% and 16% [2] of the intensity change at the measured Si interface of figure 6 is 6.49 nm. This broadening as well as the differences found in the thickness of the Si oxide interface layer measured with conventional XPS plus ion milling and with HAXPES should be attributed to the mixing effects taking place during ion bombardment. When inert energetic ions impinge on a solid surface, in addition to sputtering, there are other effects such as atomic mixing and preferential sputtering that are the main responsible for the observed changes of surface composition.

In a previous paper [16] we used ARXPS to rule out preferential sputtering effects during Ar^+ bombardment of Cr–O–Al mixed oxides grown on Si substrates. However, atomic mixing is always present in depth profile experiments by ion bombardment limiting the ultimate depth resolution. The analytical treatments of mixing are based on diffusion-like process approximations where the knock-on processes are described by random relocations [26, 27]. Only a small

fraction (∼1%) [28] of collisional relocations leads to sputter erosion and therefore atomic mixing can be assumed to redistribute the atoms within a range which is related to the projected ion range R_p. In fact, according to the solution of the diffusion equation the smearing of an originally $\delta(t)$- profile is transformed into a Gaussian distribution and a sharp interface into an error function with standard deviation [27],

$$\sigma = R\sqrt{\frac{E_\mathrm{i}}{6E_\mathrm{d}Y}}, \tag{8}$$

where R is the average distance over which a permanently displaced atom is relocated, E_i is the primary-ion energy, E_d is the displacement energy, that is the threshold energy for atomic displacement, and Y is the sputtering yield. For 1 keV Ar^+ ions and normal incidence a value of $\sigma = 4$ nm is given by Andersen [26] for Si. Since $\sigma \propto \sqrt{E_\mathrm{i}}$ a value of $\sigma = 6.9$ nm can be derived for 3 keV Ar^+ ions. Therefore, the sputter depth profile is inevitably broadened with respect to the original depth distribution by this quantity which is in good agreement with the value measured above (6.49 nm) for the broadening of the Si interface. In addition to that, Hofmann [2] pointed out that, other physical effects such as ion-beam induced roughness and information depth should contribute, in addition to atomic mixing, to the interface broadening in such a way that only the use of deconvolution methods with the appropriate resolution function or profile reconstruction methods as the MRI model [2] should allow the calculation of the 'true' Si oxide layer thickness from the sputter depth profile of figure 6. A rough estimate of the 'true' layer thickness can easily be made from figure 6. Assuming the measured FWHM of 8.2 nm for the Si oxide film and the maximum intensity around 0.25 of the bulk intensity a layer thickness of about 2 nm is obtained in fair agreement with ARXPS and HAXPES results which are not altered by ion bombardment. Consequently, we have shown that HAXPES is a powerful tool to obtain non-destructively the CDP either of buried interfaces or of thin films providing useful information that can facilitate the interpretation of physical processes as atomic mixing taking place during ion bombardment. However, to the best of our knowledge, such experiments have not been performed systematically.

4. Conclusions

A comparative study of HAXPES with the two main surface analytical techniques used to obtain chemical information and concentration depth profiles (CDPs), ARXPS and XPS and simultaneous sputtering with Ar^+, is carried out. Simple parametric models with some hypothesis about the form of the CDP have been put forward in order to explain experimental results obtained for thin-film oxides on Cr, Al, Si substrata using ARXPS and HAXPES. Both techniques are non-destructive and, within the range used for the emission angles (0–70°) and that for photon energies (7.5–15 keV), both techniques provide equivalent information, although ARXPS seems to be more sensitive to the surface morphology. XPS with simultaneous Ar^+ bombardment and HAXPES are used to explore the capabilities of analysing buried interfaces at depths above 10 nm in Cr–O–Al thin films mixed oxides deposited on Si substrata. XPS and simultaneous sputtering with Ar^+ are a destructive technique which allows obtaining the CDP but unwanted effects such as atomic mixing and induced roughness are unavoidable. In addition to that, the comparative study of both techniques supports the usefulness of HAXPES to test non-destructively such buried interfaces.

Acknowledgments

The authors would like to thank Professor R W Paynter for the fruitful discussions and comments on the manuscript. The financial support by the Ministerio de Ciencia e Innovación (MICINN) of Spain through the Consolider-Ingenio 2010 programme (CSD2008-00023) and through the project MAT2008-06618-C02 is gratefully acknowledged. The authors also thank the MICINN for provision of synchrotron radiation facilities and the BM25-Spline staff for the technical support. CP thanks the Spanish Ministerio de Educación for financial support within the Programa Nacional de Movilidad de Recursos Humanos de Investigación (PR2011-0231). REG would also like to thank the MICINN for the financial support within the Ramón y Cajal programme.

References

[1] Escobar Galindo R, Gago R, Duday D and Palacio C 2010 *Anal. Bioanal. Chem.* **396** 2725
[2] Hofmann S 1998 *Rep. Prog. Phys.* **61** 827
[3] Mao D, Wucher A and Winograd N 2010 *Anal. Chem.* **82** 57
[4] Zier M, Oswald S, Reiche R and Wetzig K 2007 *Michochim. Acta* **156** 99
[5] Palacio C, Ocón P, Herrasti P, Díaz D and Arranz A 2003 *J. Electroanal. Chem.* **545** 53
[6] Cumpson P J 1995 *J. Electron Spectrosc. Relat. Phenom.* **73** 25
[7] Paynter R W 2009 *J. Electron Spectrosc. Relat. Phenom.* **169** 1
[8] Rubio-Zuazo J and Castro G R 2008 *Surf. Interface Anal.* **40** 1438
[9] Rubio-Zuazo J and Castro G R 2005 *Nucl. Instrum. Methods* A **547** 64
[10] Shimada H, Matsubayashi N, Imamura M, Sato T and Nishijima A 1996 *Appl. Surf. Sci.* **100/101** 56
[11] Yamamoto H, Yamada Y, Sasase M and Esaka F 2008 *J. Phys.: Conf. Ser.* **100** 012044
[12] Rubio-Zuazo J and Castro G R 2011 *J. Electron Spectrosc. Relat. Phenom.* **184** 440
[13] Kövér L 2010 *J. Electron Spectrosc. Relat. Phenom.* **178/179** 241
[14] Tougaard S 1990 *J. Vac Sci Technol.* A **8** 2197
[15] Vergara L, Escobar Galindo R, Martínez R, Sánchez O, Palacio C and Albella J M 2011 *Thin Solid Films* **519** 3509
[16] Benito N, Díaz D, Vergara L, Escobar Galindo R, Sánchez O and Palacio C 2011 *Surf. Coat. Technol.* **206** 1484
[17] Rubio-Zuazo J, Escher M, Merkel M and Castro G R 2010 *Rev. Sci. Instrum.* **81** 043304
[18] Shirley D A 1972 *Phys. Rev.* B **5** 4709
[19] Proctor A and Sherwood M P A 1982 *Anal. Chem.* **54** 13
[20] Samsonov G V (Editor) 1973 *The Oxide Handbook* (New York: Plenum)
[21] Tanuma S, Powell C J and Penn C R 1994 *Surf. Interface Anal.* **21** 165

[22] McCafferty E and Wightman J P 1998 *Surf. Interface Anal.* **26** 549
[23] Kim K J and Seah M P 2007 *Surf. Interface Anal.* **39** 512
[24] Merzlikin S V, Tolkachev N N, Strunskus T, Witte G, Glogowski T, Wöll C and Grünert W 2008 *Surf. Sci.* **602** 755
[25] CASA XPS software Ltd. v2.0 User's Manual www.casaxps.com
[26] Andersen H H 1979 *Appl. Phys.* **18** 131
[27] Littmark U and Hofer W O 1984 *Thin Film and Depth Profile Analysis* (*Topics in Current Physics*) ed H Oescherner (Berlin: Springer)
[28] Wittmaack K 1991 Surface and depth analysis based on sputtering *Sputtering by Particle Bombardment III* ed R Behrisch and K Wittmaack (Berlin: Springer)